

A Four-Component Decomposition of POLSAR Image

Yoshio Yamaguchi, Motoi Ishido, Hiroyoshi Yamada

Faculty of Engineering
Niigata University
Niigata, 950-2181 Japan
yamaguchi.yoshio@ieee.org

Toshifumi Moriyama

Environment Information Technology Group
NICT
Koganei, 184-8795 Japan
toshi.moriyama@nict.go.jp

Abstract—A four-component scattering model is proposed to decompose polarimetric synthetic aperture radar images. The covariance matrix approach is used to deal with the non-reflection symmetric scattering case. This scheme includes and extends the three-component decomposition method dealing with the reflection symmetry condition that the co-pol and the cross-pol correlations are close to zero. Circular polarization power is added as the fourth component to the three component scattering model which describes surface, double bounce, and volume scattering. This circular polarization term is added to take account of the co-pol and the cross-pol correlations which generally appear in complex urban area scattering and disappear for natural distributed scatterer.

Keywords-radar polarimetry; target decomposition; covariance matrix; non-reflection symmetry; POLSAR

I. INTRODUCTION

Terrain and land use classification is one of the most important applications of Polarimetric Synthetic Aperture Radar (POLSAR) image data takes. Excellent methods have been proposed to classify terrain based on polarimetric statistical characteristics [1]-[3]. There are two major approaches for a 3x3 polarimetric matrix decomposition. One is the lexicographic Covariance matrix approach based on physically measurable parameters [1], and the other is the Coherency matrix based on mathematically orthogonal Pauli matrix components [3]. An overview on decomposition theorem is given in [3].

Three-component scattering power model [1] has been successfully applied to decompose POLSAR image under the reflection symmetry condition $\langle S_{HH} S_{HV}^* \rangle \approx 0$ and $\langle S_{VV} S_{HV}^* \rangle \approx 0$ using the covariance matrix. This method is based on simple physical scattering mechanisms (surface scattering, double bounce scattering, and volume scattering), and is powerful for POLSAR image decomposition for natural distributed target areas in the P-L-C band. The advantage of this scattering model is its simplicity and easy implementation for image processing.

However, for POLSAR image analysis including urban area scattering for which the reflection symmetry condition does not hold, it is necessary to take the effect of $\langle S_{HH} S_{HV}^* \rangle \neq 0$

and $\langle S_{VV} S_{HV}^* \rangle \neq 0$ into account. This condition is the non-reflection symmetry constraint, with which most of the research studies have not been dealing. If we examine covariance matrices in urban areas, we encounter that $\langle S_{HH} S_{HV}^* \rangle \neq 0$ and $\langle S_{VV} S_{HV}^* \rangle \neq 0$, and $\langle |S_{HV}|^2 \rangle$ is rather predominant. In order to accommodate the decomposition scheme for the more general scattering case, it is necessary to introduce another term into the model which corresponds to $\langle S_{HH} S_{HV}^* \rangle \neq 0$ and $\langle S_{VV} S_{HV}^* \rangle \neq 0$ in the covariance matrix approach.

We propose to include the circular polarization power term as the fourth component for the more general scattering mechanism. This circular polarization power term corresponds to $\langle S_{HH} S_{HV}^* \rangle \neq 0$ and $\langle S_{VV} S_{HV}^* \rangle \neq 0$, which appears in urban area whereas disappears for almost all natural distributed scattering. This term is essentially caused by the scattering matrix of helices (or equivalently, left or right circular polarization states) and is relevant for complicated shape man-made structures predominant in urban areas.

The second point is a modification of the volume scattering matrix in the decomposition according to the relative backscattering magnitudes of $\langle |S_{HH}|^2 \rangle$ versus $\langle |S_{VV}|^2 \rangle$. In the theoretical modeling of volume scattering, a cloud of randomly oriented dipole is implemented with a probability function being uniform for the orientation angles [1]. However, for vegetated areas scattering from tree trunks and branches seems to display a certain characteristic angle distribution. A modification in the orientation angle distribution is proposed for this formulation. This modification yields asymmetric matrices which can be adjusted to measurement data with $\langle |S_{HH}|^2 \rangle \neq \langle |S_{VV}|^2 \rangle$.

II. COVARIANCE MATRIX EXPANSION FOR NON-REFLECTION SYMMETRY CONDITION

To derive polarimetric scattering characteristics contained in POLSAR image, it is necessary to evaluate the second order statistics of its scattering matrices. Here, we follow the scheme [1] and present covariance matrix approach to derive a four-component scattering model mathematically. The general covariance matrix is defined as

Report Documentation Page			<i>Form Approved OMB No. 0704-0188</i>		
<p>Public reporting burden for the collection of information is estimated to average 1 hour per response, including the time for reviewing instructions, searching existing data sources, gathering and maintaining the data needed, and completing and reviewing the collection of information. Send comments regarding this burden estimate or any other aspect of this collection of information, including suggestions for reducing this burden, to Washington Headquarters Services, Directorate for Information Operations and Reports, 1215 Jefferson Davis Highway, Suite 1204, Arlington VA 22202-4302. Respondents should be aware that notwithstanding any other provision of law, no person shall be subject to a penalty for failing to comply with a collection of information if it does not display a currently valid OMB control number.</p>					
1. REPORT DATE 25 JUL 2005	2. REPORT TYPE N/A	3. DATES COVERED -			
4. TITLE AND SUBTITLE A Four-Component Decomposition of POLSAR Image			5a. CONTRACT NUMBER		
			5b. GRANT NUMBER		
			5c. PROGRAM ELEMENT NUMBER		
6. AUTHOR(S)			5d. PROJECT NUMBER		
			5e. TASK NUMBER		
			5f. WORK UNIT NUMBER		
7. PERFORMING ORGANIZATION NAME(S) AND ADDRESS(ES) Faculty of Engineering Niigata University Niigata, 950-2181 Japan		8. PERFORMING ORGANIZATION REPORT NUMBER			
9. SPONSORING/MONITORING AGENCY NAME(S) AND ADDRESS(ES)			10. SPONSOR/MONITOR'S ACRONYM(S)		
			11. SPONSOR/MONITOR'S REPORT NUMBER(S)		
12. DISTRIBUTION/AVAILABILITY STATEMENT Approved for public release, distribution unlimited					
13. SUPPLEMENTARY NOTES See also ADM001850, 2005 IEEE International Geoscience and Remote Sensing Symposium Proceedings (25th) (IGARSS 2005) Held in Seoul, Korea on 25-29 July 2005. , The original document contains color images.					
14. ABSTRACT					
15. SUBJECT TERMS					
16. SECURITY CLASSIFICATION OF:			17. LIMITATION OF ABSTRACT UU	18. NUMBER OF PAGES 4	19a. NAME OF RESPONSIBLE PERSON
a. REPORT unclassified	b. ABSTRACT unclassified	c. THIS PAGE unclassified			

$$\langle [C] \rangle^{HV} = \begin{bmatrix} \langle |S_{HH}|^2 \rangle & \sqrt{2} \langle S_{HH} S_{HV}^* \rangle & \langle S_{HH} S_{VV}^* \rangle \\ \sqrt{2} \langle S_{HV} S_{HH}^* \rangle & 2 \langle |S_{HV}|^2 \rangle & \sqrt{2} \langle S_{HV} S_{VV}^* \rangle \\ \langle S_{VV} S_{HH}^* \rangle & \sqrt{2} \langle S_{VV} S_{HV}^* \rangle & \langle |S_{VV}|^2 \rangle \end{bmatrix} \quad (1)$$

where $\langle \cdot \rangle$ denotes the ensemble average in the data processing; and the superscript $*$ denotes complex conjugation. Under the non-reflection symmetry condition, $\langle S_{HH} S_{HV}^* \rangle \neq 0$ and $\langle S_{VV} S_{HV}^* \rangle \neq 0$, we have all non-zero terms. Since most of the works have been dealing with the reflection symmetry condition, $\langle S_{HH} S_{HV}^* \rangle^a \langle S_{VV} S_{HV}^* \rangle^a \neq 0$, we have to develop the corresponding scattering term. The basic scattering mechanism related to the non-reflection condition is found to be helicity (or equivalently, circular polarization state) of which covariance form is given as

$$\begin{aligned} \langle [C] \rangle_{r-helix}^{hv} &= \frac{1}{4} \begin{bmatrix} 1 & j\sqrt{2} & -1 \\ -j\sqrt{2} & 2 & j\sqrt{2} \\ -1 & -j\sqrt{2} & 1 \end{bmatrix} \quad \text{or} \\ \langle [C] \rangle_{l-helix}^{hv} &= \frac{1}{4} \begin{bmatrix} 1 & -j\sqrt{2} & -1 \\ j\sqrt{2} & 2 & -j\sqrt{2} \\ -1 & j\sqrt{2} & 1 \end{bmatrix} \end{aligned} \quad (2)$$

This helix (circular polarization) term is assigned to the fourth component of scattering mechanism. Since the Trace of (2) is unity, the corresponding power can be given by taking average of a measured covariance matrix as

$$\frac{f_c}{4} = \frac{1}{2} \left| \text{Im} \{ \langle S_{HH} S_{HV}^* \rangle + \langle S_{HV} S_{VV}^* \rangle \} \right| \quad (3)$$

where f_c is the coefficient to the unit power. The scattering power is based on the trace of covariance matrix.

III. FOUR-COMPONENT SCATTERING POWER DECOMPOSITION

We expand the measured covariance matrix using a four scattering model, namely, surface scattering, double bounce scattering, volume scattering, and the circular polarization power term as follows:

$$\begin{aligned} \langle [C] \rangle^{HV} &= f_s \langle [C] \rangle_{surface}^{hv} + f_d \langle [C] \rangle_{double}^{hv} \\ &\quad + f_v \langle [C] \rangle_{vol}^{hv} + f_c \langle [C] \rangle_{circular}^{hv} \\ &= f_s \begin{bmatrix} |b|^2 & 0 & b \\ 0 & 0 & 0 \\ b^* & 0 & 1 \end{bmatrix} + f_d \begin{bmatrix} |a|^2 & 0 & a \\ 0 & 0 & 0 \\ a^* & 0 & 1 \end{bmatrix} \\ &\quad + f_v \langle [C] \rangle_{vol}^{hv} + \frac{f_c}{4} \begin{bmatrix} 1 & \pm j\sqrt{2} & -1 \\ \mp j\sqrt{2} & 2 & \pm j\sqrt{2} \\ -1 & \mp j\sqrt{2} & 1 \end{bmatrix} \end{aligned} \quad (4)$$

where the first and the second terms are identical with those in [1]. For the third term, $\langle [C] \rangle_{vol}^{hv}$, we choose one of the

following covariance matrices according to the relative measurement value of $\langle |S_{HH}|^2 \rangle$ and $\langle |S_{VV}|^2 \rangle$

$$\begin{aligned} \langle [C] \rangle_{vol}^{hv} &= \frac{1}{15} \begin{bmatrix} 8 & 0 & 2 \\ 0 & 4 & 0 \\ 2 & 0 & 3 \end{bmatrix}, \quad \langle [C] \rangle_{vol}^{hv} = \frac{1}{8} \begin{bmatrix} 3 & 0 & 1 \\ 0 & 2 & 0 \\ 1 & 0 & 3 \end{bmatrix}, \\ \langle [C] \rangle_{vol}^{hv} &= \frac{1}{15} \begin{bmatrix} 3 & 0 & 2 \\ 0 & 4 & 0 \\ 2 & 0 & 8 \end{bmatrix}. \end{aligned} \quad (5)$$

These matrices are derived by the second order statistics for randomly oriented wires with appropriate probability density functions considering actual tree distribution. This choice allows us to make a straightforward best-fit to the measured data $\langle |S_{HH}|^2 \rangle \neq \langle |S_{VV}|^2 \rangle$.

Comparing the matrix elements yields the following 5 equations with 6 unknowns a, b, f_s, f_d, f_v and f_c

$$\langle |S_{HH}|^2 \rangle = f_s |b|^2 + f_d |a|^2 + \frac{8}{15} f_v + \frac{f_c}{4} \quad (6a)$$

$$\langle |S_{HV}|^2 \rangle = \frac{2}{15} f_v + \frac{f_c}{4} \quad (6b)$$

$$\langle |S_{VV}|^2 \rangle = f_s + f_d + \frac{3}{15} f_v + \frac{f_c}{4} \quad (6c)$$

$$\langle S_{HH} S_{VV}^* \rangle = f_s b + f_d a + \frac{2}{15} f_v - \frac{f_c}{4} \quad (6d)$$

$$\frac{1}{2} \{ \langle S_{HH} S_{HV}^* \rangle + \langle S_{HV} S_{VV}^* \rangle \} = j \frac{f_c}{4}. \quad (6e)$$

Since the left hand side of (6) is a measurable quantity, we can determine f_c directly with the aid of (3).

$$\begin{aligned} f_c &= P_c = 2 \left| \text{Im} \{ \langle S_{HH} S_{HV}^* \rangle + \langle S_{HV} S_{VV}^* \rangle \} \right| \\ &= 2 \left| \text{Im} \langle S_{HV}^* (S_{HH} - S_{VV}) \rangle \right| \end{aligned} \quad (7)$$

Then, (6b) gives the volume scattering coefficient f_v directly as

$$f_v = \frac{15}{2} \left(\langle |S_{HV}|^2 \rangle - \frac{f_c}{4} \right) \quad (8)$$

The remaining 4 unknowns with 3 equations can be obtained in the same manner as shown in [1]. The scattering powers, P_s, P_d, P_v , and P_c , corresponding to surface, double bounce, volume, and circular polarization contributions, respectively, are obtained as

$$P_s = f_s (1 + |b|^2), \quad P_d = f_d (1 + |a|^2), \quad P_v = f_v, \quad P_c = f_c \quad (9)$$

$$P_t = P_s + P_d + P_v + P_c = \langle |S_{HH}|^2 + 2 |S_{HV}|^2 + |S_{VV}|^2 \rangle. \quad (10)$$

The above equations (5)-(10) are the main set of expressions for the four-component decomposition.

IV. DECOMPOSITION ALGORITHM

When we apply the four component decomposition scheme to POLSAR data directly, we sometimes encounter a problem in that the coefficients f_s or f_d become negative for certain areas. Since the negative coefficient indicates the

corresponding power is negative, it is inconsistent with the physical phenomenon. A typical feature of such areas is that $\langle |S_{HV}|^2 \rangle$ is rather predominant compared to $\langle |S_{HH}|^2 \rangle$ and to $\langle |S_{VV}|^2 \rangle$. These areas reside within small sections of geometrically complicated man-made scattering (cultivated) and of forested areas. In order to avoid such inconsistency, we devised an algorithm for the four-component decomposition which could be applied to general POLSAR data image analyses.

The main point for avoiding the inconsistency is to use the following power ratio:

$$2 \langle |S_{HV}|^2 \rangle : \langle |S_{HH}|^2 \rangle \text{ or } \langle |S_{VV}|^2 \rangle \quad (11)$$

based on statistics [3]-[4] and on our experiences of POLSAR image analysis [5]. The theoretical studies showed that co-pol radar channel power and cross-pol channel power are of the magnitude ratio of 2:1 statistically [3]-[4]. This condition is used in the middle stage of the four-component decomposition algorithm in Fig.1

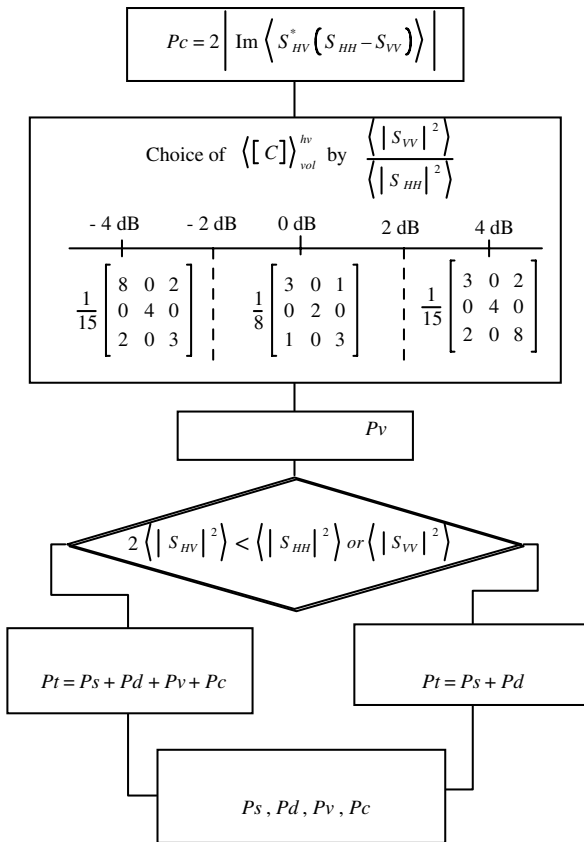


Figure 1. Decomposition Algorithm for four component decomposition.

V. EXAMPLE

An X-band Pi-SAR data set was used for the four-component decomposition. The Pi-SAR sensor is an airborne POLSAR system developed by NICT and JAXA of Japan. The resolution in the X-band image is 1.5 m by 1.5 m. The area chosen for analysis is Yamakoshi village, Niigata, Japan, which has been suffered from a big earthquake occurred on Oct. 23, 2004. The Pi-SAR collected fully polarimetric data over these areas on Oct. 26 and Nov. 3. An aerial photo on Oct. 28 is shown in Fig.2 for reference. A color coded image resulted from the four component decomposition with P_s (blue), P_d (red), and P_v (green) is shown in Fig.3.

It is seen that residential houses (red: center in Fig.3) can be easily recognized by the decomposition because these man-made targets exhibit double bounce reflections. Therefore POLSAR image has advantage in identifying the man-made targets using color code compared to the photo (Fig.2) in which these houses are often missed by eye.

Since one of the authors was born and grown up in this village, it was easy to verify the decomposition result which was consistent with physical scattering phenomena.

Fig.3(a) and (b) show temporal image series. As can be seen in the middle right portion of (a), there is a dark region. This region was caused by water pod (small dam) at the beginning of the earthquake. On the other hand, it disappeared in (b) due to run-off during the data take. It is seen in (b) that the volume power component P_v is generated again in the corresponding area.

The fourth component, P_c , is shown in Fig.4. This term is generated from houses, man-made structures and facets of strong reflections. The power is small compared to P_s , P_d , P_v .

VI. CONCLUSION

A four-component scattering model based on the covariance matrix is presented for polarimetric SAR data decomposition. The four components are single bounce, double bounce, volume scattering and circular polarization powers. The decomposition scheme incorporates non-reflection symmetry condition which has not been dealt with. The fourth component, circular polarization power, corresponds to the imaginary part of $\langle S_{HH} S_{HV}^* \rangle$ which often appears in complex urban area and disappears in natural distributed target. The volume scattering symmetric and asymmetric covariance can be chosen to fit the relative magnitude between $\langle |S_{HH}|^2 \rangle$ and $\langle |S_{VV}|^2 \rangle$ of measurement data. This decomposition is applied to an disaster area by earthquake using X-band Pi-SAR image.

ACKNOWLEDGMENT

The authors are grateful for the Pi-SAR image data taken collected and provided by NICT and JAXA, Japan. The work was supported in part by the Grant in Aid for Scientific



Figure 2. Photo (Tanesuhara, Yamakoshi village: Oct.28, 2004)

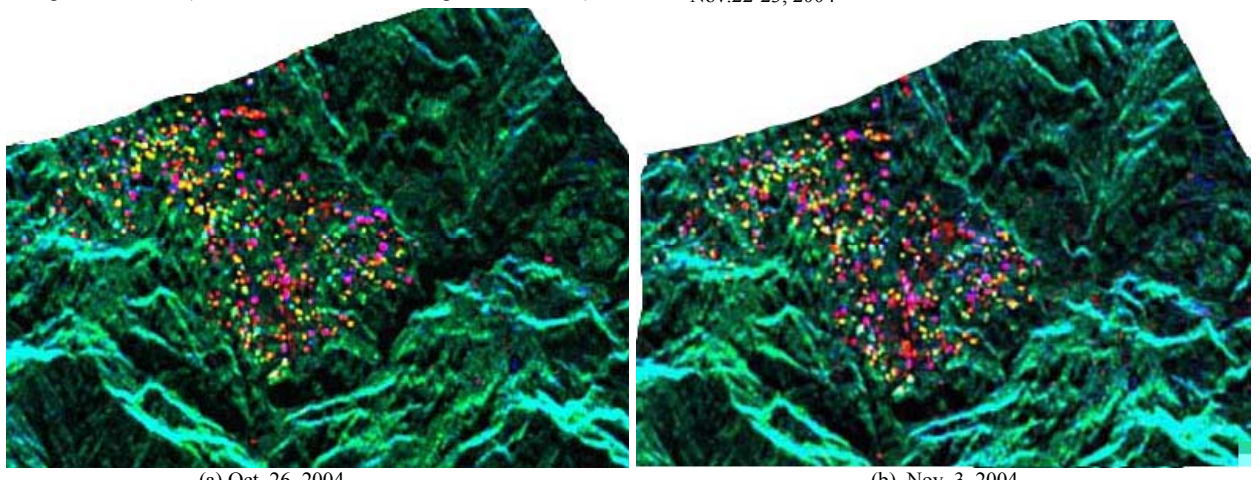


Figure 3. Decomposed and color coded image of Yamakoshi village : Ps (blue), Pd (red), and Pv (green)
Chuetsu earthquake occurred on October 23, 2004.

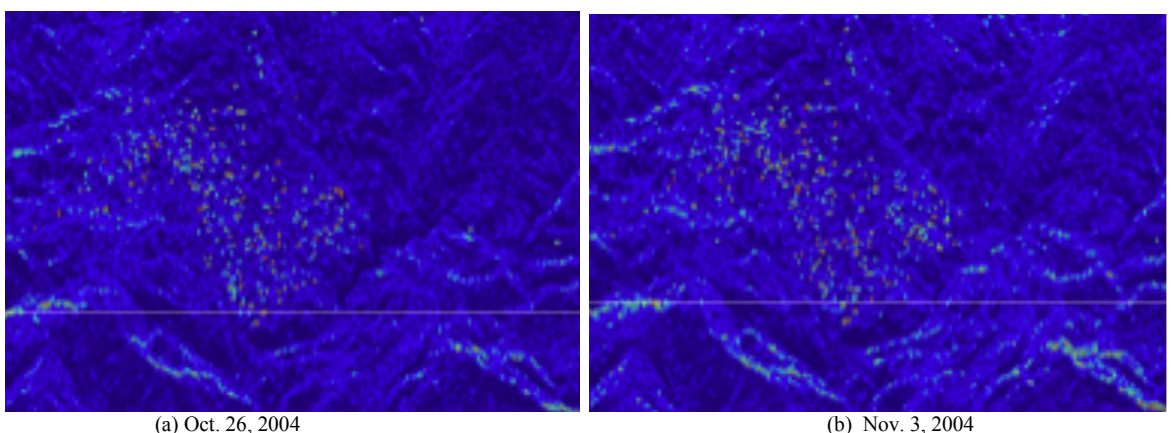


Figure 4. Circular polarization power P_c

REFERENCES

- [1] A. Freeman and S. L. Durden, "A three-component scattering model for polarimetric SAR data," *IEEE Trans. Geoscience Remote Sensing*, vol.36, no.3, pp.963-973, 1998
- [2] S. R. Cloude and E. Pottier, "A review of target decomposition theorems in radar polarimetry," *IEEE Trans. Geoscience Remote Sensing*, vol.34, no.2, pp.498-518, 1996
- [3] Y. Ke, "Notes on invariant characters of radar cross sections," *2001 CIE Int'l Conference on Radar Proc.*, pp.418-422, 2001.
- [4] Jian Yang, Ph.D dissertation, "On theoretical problems in radar polarimetry," Graduate School of Science and Technology, Niigata University, Japan, 2000.
- [5] Y. Yamaguchi, T. Moriyama, M. Ishido, H. Yamada, "Four Component Scattering Model for Polarimetric SAR Image Decomposition," *Proc. of 2004 Korea-Japan Joint Conference on AP/EMC/EMT*, pp.105-108, Nov.22-23, 2004